Journal of
Materials Chemistry A

Accepted Manuscript

Volume 4 | Number 1 | 7 January 2016 | Pages 1–330

Journal of
Materials Chemistry A

Materials for energy and sustainability
www.rsc.org/MaterialsA

ISSN 2050-7488

ROYAL SOCIETY OF CHEMISTRY

PAPER
Kun Chang, Zhaorong Chang et al.
Bubble-template-assisted synthesis of hollow fullerene-like
MoS₂ nanocages as a lithium ion battery anode material

175 YEARS

This is an Accepted Manuscript, which has been through the Royal Society of Chemistry peer review process and has been accepted for publication.

Accepted Manuscripts are published online shortly after acceptance, before technical editing, formatting and proof reading. Using this free service, authors can make their results available to the community, in citable form, before we publish the edited article. We will replace this Accepted Manuscript with the edited and formatted Advance Article as soon as it is available.

You can find more information about Accepted Manuscripts in the author guidelines.

ROYAL SOCIETY
OF CHEMISTRY

rsc.li/materials-a

Journal Name

ARTICLE
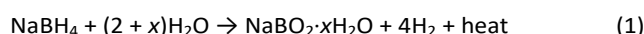
Realizing Facile Regeneration of spent NaBH₄ with Mg-Al Alloy

Hao Zhong[a], Liuzhang Ouyang[a,b]*, Meiqin Zeng[a], Jiangwen Liu[a], Hui Wang[a], Huaiyu Shao[c]*, Michael Felderhoff[d,*], Min Zhu[a]

The regeneration of sodium borohydride (NaBH₄) is crucial to form a closed cycle after it either supplies hydrogen energy via hydrolysis process, or provides energy through electron transfer at anode of direct borohydride fuel cells (DBFCs). In both of these cases, the spent fuels are NaB(OH)₄ from NaBO₂ aqueous solution. However, the current regeneration process from (NaB(OH)₄)·xH₂O to form NaBH₄ by reduction reaction and calcination at high temperature with metal hydrides as reducing agents is a very expensive and costly process. In this work we developed a simple regeneration process via ball milling with Mg-Al alloys as reducing agent for (NaB(OH)₄) under argon atmosphere. Under optimized conditions a high yield of about 72% of NaBH₄ could be obtained. Mechanism study shows that all hydrogen atoms from (NaB(OH)₄) remains in NaBH₄ and no additional hydrogen sources are needed for the reduction process. The inexpensive Mg-Al alloy works as reducing agent transforming the H⁺ to H⁻ in NaBH₄. This approach demonstrates a ~20-fold cost reduction compared with the method using metal hydrides. This opens a door to a commercial implementation of simple ball-milling processes for the regeneration of spend NaBH₄ from NaBO₂ H₂O with cheap reducing agents.

1. Introduction

Fuel cells provide a promising alternative technology for electrical power generation from renewable energy carrier, for instance, hydrogen energy.[1] However, currently fuel supply is still one of the biggest hindrances for worldwide applications of mobile fuel cell technologies.[2, 3] Hydrogen supply via hydrolysis of sodium borohydride (NaBH₄)[4] and direct borohydride fuel cells (DBFCs) possess great potentials as possible solutions.[5] But both of these technologies are facing the issue of suffering from the high cost of NaBH₄, as well as the difficulties in the regeneration of the spent fuel [6, 7]. Therefore, a high efficiency and low cost approach for a simple regeneration process of spent NaBH₄ is highly desirable. This could be the key step and enabling technology for further distribution of NaBH₄ powered fuel cell applications.

The spent fuel of NaBH₄ hydrolysis is confirmed by the following hydrolysis reaction:

$$NaBH_4 + (2 + x)H_2O \rightarrow NaBO_2 \cdot xH_2O + 4H_2 + heat \qquad (1)$$

where x is the hydration factor.[8] However, it should be noted that the spent fuel is normally hydrated sodium metaborate (NaBO₂) or its aqueous solution after the hydrolysis.[9] And the actual formula of NaBO₂·2H₂O and NaBO₂·4H₂O are NaB(OH)₄ and NaB(OH)₄·2H₂O,respectively, according to the chemical structures.[10] In DBFCs, NaBH₄ is oxidized at the anode according to the following reaction:

$$BH_4^- + 8OH^- \rightarrow BO_2^- + 6H_2O + 8e^-,$$
$$E^0 = -1.24 \text{ V vs. SHE} \qquad (2)$$
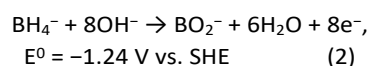
The spent fuel of the anode reaction is B(OH)₄⁻ and H₂O, which are generated also as a NaBO₂ aqueous solution.[7, 11] From NaBO₂ aqueous solution, NaB(OH)₄·2H₂O or NaB(OH)₄ can be obtained via drying treatment at temperature of < 54 °C or 54 − 110 °C, respectively; while dehydrated NaBO₂ can be formed after treatment at temperature > 350 °C.[12] Over the past decades, a great deal of efforts has been made toward dehydrated NaBO₂ reduction. With a calcination treatment at 550 °C, MgH₂ reduced the dehydrated NaBO₂ to NaBH₄ under hydrogen pressure.[13] Ball milling with metal hydrides at near room temperature can also achieve the reduction under argon atmosphere with a NaBH₄ yield of over 70 %.[14-16] However, the synthesis of metal hydrides at high temperature could be one important factor in energy consuming and costs. Without usage of metal hydrides, high temperature annealing treatment under hydrogen pressure for Mg[13, 17], Mg and Si[13] or transition metals (Fe, Co or Ni)[18, 19] mixed with dehydrated NaBO₂ is another reduction technique. But this high

a. School of Materials Science and Engineering, Guangdong Provincial Key Laboratory of Advanced Energy Storage Materials, South China University of Technology, Guangzhou, 510641, People's Republic of China

b. China-Australia Joint Laboratory for Energy & Environmental Materials, Key Laboratory of Fuel Cell Technology of Guangdong Province, Guangzhou, 510641, People's Republic of China.

c. Joint Key Laboratory of the Ministry of Education, Institute of Applied Physics and Materials Engineering (IAPME), University of Macau, Macau SAR, China.

d. Max-Planck-Institut für Kohlenforschung, 45470 Mülheim an der Ruhr, Germany

† Footnotes relating to the title and/or authors should appear here.
Electronic Supplementary Information (ESI) available: XRD analysis of the raw materials; XRD analysis of the ball milled products; XPS analysis of the ball milled raw material; Cost calculation of raw materials for NaBH₄ produced by different approaches. See DOI: 10.1039/x0xx00000x

temperature dehydration process of $NaBO_2$ is also energy consuming and additional hydrogen supply is needed, which increases the costs of the regeneration process (hydrogen from renewable sources, like water splitting or unsustainably from fossil fuels). Direct reduction of hydrated $NaBO_2$ with Mg by annealing at 3 MPa hydrogen pressure may be one of the options, but the yield is only 12.3 % of $NaBH_4$[20]. Therefore, an innovative low-cost and high-efficiency approach of $NaBH_4$ regeneration is of great importance and it is urgently required.

Herein, instead of only Mg, we introduce aluminum (Al) in the reduction process of hydrated $NaBO_2$ because it can offer more electrons than Mg but with similar reducibility, which may further decrease the cost and increase the yield of the process. In addition, Mg and Al are relatively soft metal making the ball milling process less efficient. Thus, magnesium aluminum alloy ($Mg_{17}Al_{12}$) was chosen as a reducing agent in this work. The alloy was used to react with hydrated $NaBO_2$ via ball milling under argon atmosphere in order to regenerate $NaBH_4$. During the ball milling process oxide layers on the alloy will be destroyed and fresh surfaces are always produced during the milling. This will increase the overall kinetics of the regeneration process.

In this process, the $Mg_{17}Al_{12}$ alloy offers a higher $NaBH_4$ yield and a lower cost, while the hydrated $NaBO_2$ provides a self-sufficient hydrogen source with no need of any additional hydrogen input. Furthermore, the unnecessity of drying at high temperature (> 350 °C) may greatly reduce energy consumption during the regeneration process. Therefore, this regeneration approach of $NaBH_4$ may be a very promising solution for future energy supply technologies.

2. Experimental

2.1 Chemicals

$Mg_{17}Al_{12}$ was purchased from Aike Reagent (China), while $NaB(OH)_4$ was obtained by drying $(NaB(OH)_4)\cdot 2H_2O$ (> 99 %, Sigma-Aldrich) for 12 h. Ethylenediamine (≥ 99 %) was purchased from Sigma-Aldrich. The chemicals for quantification, potassium iodate (KIO_3, AR grade), H_2SO_4 (98 %), NaOH (≥ 99 %), starch indicator (≥ 99 %), and sodium thiosulfate solution ($Na_2S_2O_3$, 1 M, AR grade) were purchased from Aladdin, and potassium iodide (KI, ≥ 99 %) were purchased from TCI. The $Mg_{17}Al_{12}$ and the generated $NaB(OH)_4$ were stored and handled in an argon filled glove box (Mikrouna, China). The oxygen and water concentrations in the glove box were always below 1 ppm.

2.2 $NaBH_4$ regeneration

For a typical experiment, totally 1 g of $Mg_{17}Al_{12}$ and $NaBO_2\cdot 2H_2O$ with different mole ratios and 50 g of steel balls (ball to powder ratio of 50 : 1, 4 steel ball of 10 mm and 68 steel ball of 6 mm) were mixed and loaded in the milling vial in the glove box. Then, the ball milling reactions were carried out in a shaker mill (QM-3C, Nanjing, China) at 1200 cycles per min (cpm).

2.3 Purification and quantification

A 20 mL of ethylenediamine was used to extract $NaBH_4$ from the ball milled products. The turbid solution was then filtrated via a polytetrafluoroethylene filter. The clear $NaBH_4$ solution was dried via a freeze dryer (Martin Christ, Alpha 1-2LD Plus, Germany) to obtain $NaBH_4$ as white powder and the waste solvent (ethylenediamine) collected in the cold trap. The purified $NaBH_4$ was quantified by the iodate method.[21] The yield of $NaBH_4$ was calculated according to the following equation:

$$Yield = \frac{obtained\ NaBH_4\ mass}{theoretical\ NaBH_4\ mass} \times 100\% \qquad (3)$$

2.4 Hydrolysis process

Hydrolysis test was conducted via a hydrolysis apparatus introduced here.[22] In each hydrolysis experiment, 0.1 g of $NaBH_4$ was used to react with 0.225 mL of a 5 wt% aqueous solution of $CoCl_2$ at room temperature and the hydrogen generation curves were automatically collected.

2.5 Characterization

Phase composition was measured via X-ray diffractometer (XRD, Rigaku MiniFlex 600) with Cu Kα radiation (λ = 1.5406 Å) at 45 kV and 40 mA. Because both of the raw materials and milling products are air sensitive, liquid paraffin was used to protect the XRD samples from air. Chemical bonds of the products were measured via Fourier-transform infrared spectroscopy (FTIR, IS50, Nicolet) in transmission mode. Potassium bromide (KBr) pellets for FTIR measurements were prepared in the glove box with a sample to KBr ratio of 1:99. The ball milling products were also characterized by solid-state ^{11}B magic-angle spinning nuclear magnetic resonance (MAS NMR) spectroscopy (AVANCE III HD 400, Bruker. Scanning electron microscopy (SEM; Supra-40, Zeiss) was used to characterize the morphology of $NaBH_4$.

3. Results and discussion

3.1 $NaBH_4$ synthesis

For the $NaBH_4$ regeneration, a mixture of $Mg_{17}Al_{12}$ alloy and $NaB(OH)_4$ in a molar ratio of 4 : 35 was mechanochemically treated with a ball to powder ratio of 50 : 1 at 1200 cpm under argon atmosphere. The XRD curves of the raw materials are shown in Fig. S1. Fig. 1a shows the XRD curves of the generated $NaBH_4$ after milling depending on the milling time. It can be seen that the raw materials ($Mg_{17}Al_{12}$ and ($NaB(OH)_4$)) lose their intensity gradually with increasing milling time. The (200) diffraction peak of $NaBH_4$ at around 28.9° in the XRD pattern confirms the generation of $NaBH_4$ after two hours of milling. With the further increase of milling time, diffraction peak of $NaBH_4$ becomes stronger after 5 h milling but the intensity decrease after 10 h milling, which may result from the combination effect of amorphization and $NaBH_4$ generation during ball milling. After 20 h milling, (111) and

(220) diffraction peaks of NaBH$_4$ at around 25.1° and 41.4° appear with the sharper (200) diffraction peak at 28.9°

commercial NaBH$_4$. Therefore, we may conclude that the regenerated NaBH$_4$ with similar crystal structure and bonding
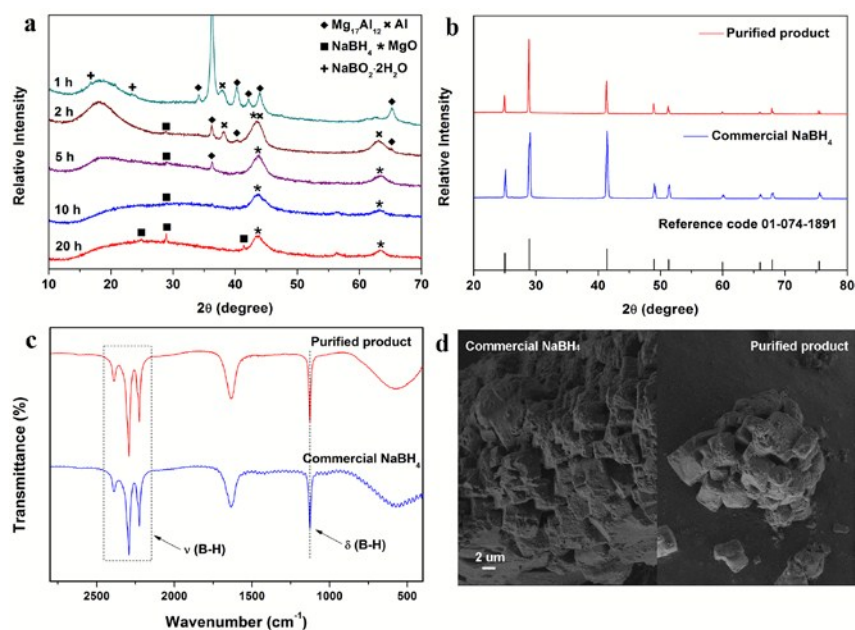
Fig. 1. (a) XRD patterns of the 5, 7.5, 10 and 20 h ball milled products of Mg$_{17}$Al$_{12}$ and NaB(OH)$_4$ mixtures (in a 4 : 35 molar ratio). (b) XRD patterns of the purified product (red line) and commercial NaBH$_4$ (blue line). (c) FTIR spectra of the purified product (red line) and commercial NaBH$_4$ (blue line). (d) SEM images of the commercial NaBH$_4$ (left) and the purified product (right).
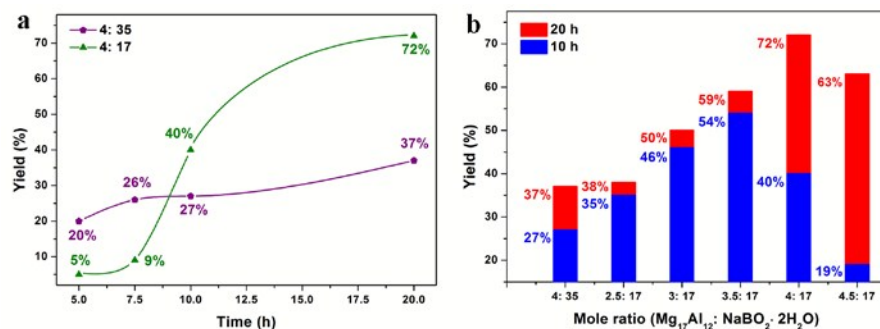

Fig. 2. (a) Yields of the ball milled products of Mg$_{17}$Al$_{12}$ and NaB(OH)$_4$ mixtures (in 4 : 35 and 4 : 17 molar ratio) for different milling time. (b) Yields of the 10 and 20 h ball milled products of Mg$_{17}$Al$_{12}$ and NaB(OH)$_4$ mixtures with different mole ratios.

because of the crystallization.[23]

To remove the byproducts from the powder after 5 h milling and obtain high purity NaBH$_4$, the ball milling products were further purified. Fig. 1b presents the XRD curves for the purified NaBH$_4$ product and in comparison to the commercial material. As compared to the one from commercial NaBH$_4$, the similar diffraction pattern of the purified NaBH$_4$ and the sharp (111), (200), (220), (311), (222), (400), (331) and (420) diffraction peaks[14, 15] indicate the successful generation of high purity NaBH$_4$ phase. No other reflections can be detected from the XRD pattern. From the FTIR spectra of these two samples shown in Fig. 1c, the bonds of the purified NaBH$_4$ were further analyzed. The stretching (2200-2400 cm^{-1}) and bending (1125 cm^{-1}) vibrations of B-H appear in the spectrum of the purified NaBH$_4$,[14, 16] which are similar to the vibrations of

feature as the commercial one was regenerated by the reaction between Mg$_{17}$Al$_{12}$ and NaB(OH)$_4$ via ball milling. This method not only avoids high temperature process of 350 °C for NaB(OH)$_4$ reduction, but also realizes the complete H supply for the regenerated NaBH$_4$ from the [OH]$^-$ group of NaB(OH)$_4$. Fig. 1d shows the SEM images of the purified NaBH$_4$ and the commercial one. The grain like surface structure in the purified NaBH$_4$ is quite similar to the commercial NaBH$_4$, which indicates that the regenerated NaBH$_4$ shows almost a similar surface morphology to the commercial NaBH$_4$.

3.2 Yield

Fig. 2a presents the yields of high-purity NaBH$_4$ prepared from the raw materials Mg$_{17}$Al$_{12}$ and NaB(OH)$_4$ in a molar ratio of 4 : 35 and 4 : 17 depending on the milling time. Quantification
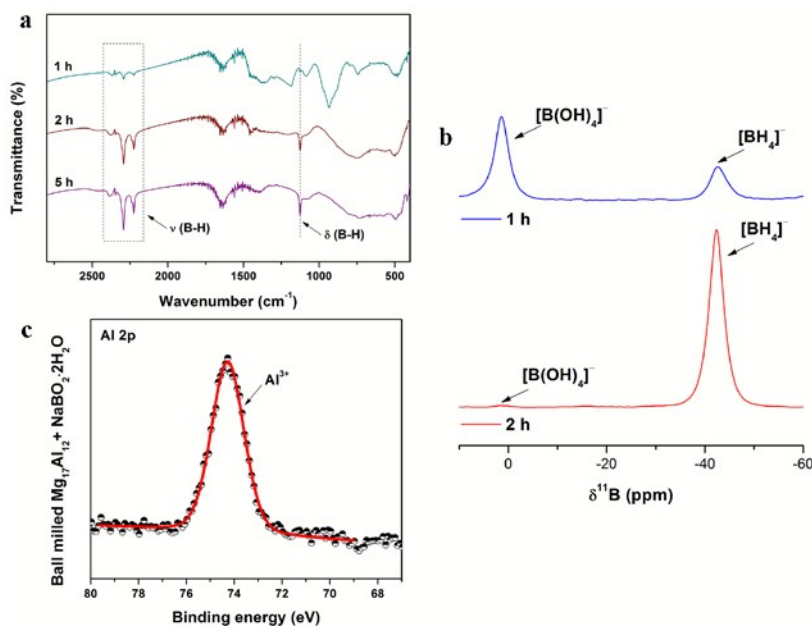
Fig. 3. (a) FTIR spectra of the 1, 2 and 5 h ball milled products of $Mg_{17}Al_{12}$ and $NaB(OH)_4$ mixtures (in a molar ratio of 4 : 35). (b) ^{11}B NMR spectra of the 1 and 2 h ball milled products of $Mg_{17}Al_{12}$ and $NaB(OH)_4$ mixtures (in a 4 : 35 molar ratio). (c) XPS spectra of Al 2p of the 1 h ball milled products of $Mg_{17}Al_{12}$ and $NaB(OH)_4$ mixtures (in a 4 : 35 molar ratio).

of the pure $NaBH_4$ was done with the iodate method. . For the 4 : 35 ratio, the $NaBH_4$ yield after 5 h milling is 20 % and the yields increase with the milling time. After 20 h milling the yield reaches a value of 37 %. As known from previous studies the relation of $NaB(OH)_4$ to the reduction compound has an important influence on the $NaBH_4$ yield.[24-26] It was further optimized by varying the molar ratio of $Mg_{17}Al_{12}$ and $NaB(OH)_4$ (raw materials ratio). Fig. 2b shows the results of $NaBH_4$ yields depending on the raw materials ratio from 4 : 35 to 4.5 : 17 after 10 and 20 h ball milling. In both of the milling durations, the $NaBH_4$ yields first increase then decrease with the increasing raw materials ratios. However, the highest yield after 10 h ball milling is 54 % with the raw materials ratio of 3.5 : 17, while that of 20 h milling is 72 % when the raw materials ratio is 4 : 17. It should be noted that the highest $NaBH_4$ yield in this work of 72 % is higher than the yield of Mg and $NaB(OH)_4$ system in our previous study[27] and also approaches to the ones from others' work of $NaBH_4$ regeneration via MgH_2 and $NaBO_2$.[14-16] The yields for the shorter milling times of the products with raw materials ratio of 4 : 17 are presented in Fig. 2a. The yields of 5 h (5 %) and 7.5 h (9 %) are lower than that with 4 : 35 raw molar ratio, and the diffraction peaks of $NaBH_4$ can not be found in the XRD results (Fig. S2). Diffraction peaks of $NaBH_4$ appear in the pattern of the product after 5 h ball milling, while the peak of $NaBH_4$ appears in the pattern of the product with 4 : 35 raw materials ratio only after 2 h ball milling (Fig. 1a). A strong crystallization of $NaBH_4$ happens when the ball milling time increases to 20 h. The diffraction peaks of $NaBH_4$ in the product with raw materials ratio of 4 : 17 become much sharper (Fig. S2).

3.3 Reaction mechanism

To clarify the reaction mechanism between $Mg_{17}Al_{12}$ alloy and $NaB(OH)_4$, the products of different milling times were also investigated and characterized with FTIR as shown in Fig. 3a. According to the XRD patterns in Fig. 1a, the (111) diffraction peak of Al at 38.4° and the (200) diffraction peak of MgO at 42.9° imply the generation of Al and MgO after 1 and 2 h milling. After 1 h milling, the formation of $NaBH_4$ could be verified by the appearance of B-H vibrations in the FTIR spectrum in Fig. 3a and the $[BH_4]^-$ resonance from Fig. 3b. According the NMR spectra (Fig. 3b), $[B(OH)_4]^-$ is gradually reduced to $[BH_4]^-$ in this process. Therefore, the first step of the regeneration process can be described by the following reaction:

$$Mg_{17}Al_{12} + NaB(OH)_4 \rightarrow MgO + Al + NaBH_4 \qquad (4)$$
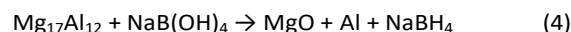
The diffraction peaks of Al then disappear after 5 h milling, which indicates that Al may become amorphous or work as a reducing agent and react with $NaB(OH)_4$ during ball milling. Because Al was generated after 1 h milling and was possible to react with $NaB(OH)_4$, to further confirm the reaction, the product was characterized by XPS and the result is shown in Fig. 3c, which may provide more evidence. The only peak which appears at 74.30 eV in the spectrum is indexed to Al^{3+}, while peak belonging to Al^0 in $Mg_{17}Al_{12}$ can be found in the spectra of the $Mg_{17}Al_{12}$ (Fig. S3) milled with the same parameters. These evidences indicate that Al reacts with $NaB(OH)_4$ in this reaction. To further unveil the reaction mechanism, pure Al-metal and $NaB(OH)_4$ in a molar ratio of 24 : 9 were ball milled for 5 h with the same other milling parameters. Only diffraction peaks from Al-metal are found in

Journal of Materials Chemistry A Accepted Manuscript

the XRD pattern (Fig. S4a) and on the other hand, B-H vibrations appear in the FTIR spectrum (Fig. S4b). This demonstrates that even Al-metal can react with $NaB(OH)_4$ producing $NaBH_4$. Considering Mg transfers to MgO in this system, it can be assumed that the byproduct is Al_2O_3 but not $Al(OH)_3$, which may be amorphous so that its diffraction peaks can not be observed in the XRD patterns. Therefore, the reaction of the second step is described as:
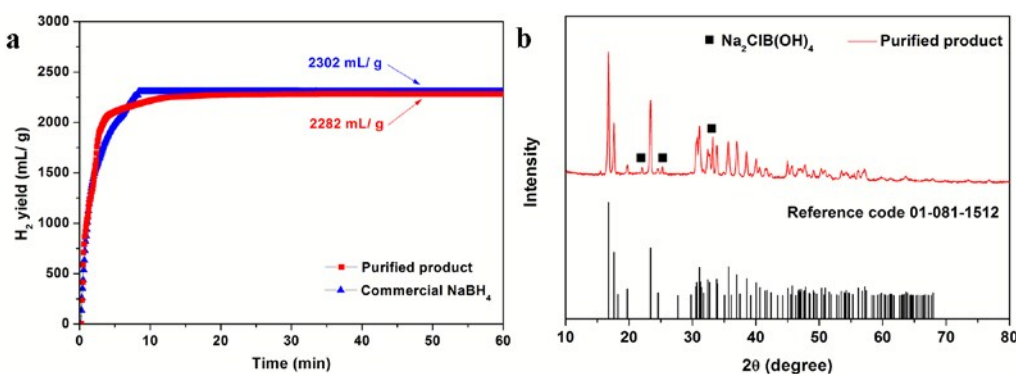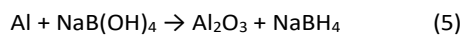
$$Al + NaB(OH)_4 \rightarrow Al_2O_3 + NaBH_4 \qquad (5)$$

located at 22.0°, 25.2° and 33.2° are indexed to the (101), (111) and (211) of $Na_2ClB(OH)_4$, while other peaks are similar as the ones of $NaB(OH)_4$. We may conclude here that the $NaB(OH)_4$ is the main phase of the byproduct, which can be regenerated by the above method.

Conclusion

In summary, $NaB(OH)_4$ can be successfully reduced with $Mg_{17}Al_{12}$ alloy via ball milling to realize a very easy

Fig. 4. (a) Hydrolysis curves of the purified product (red line) and commercial $NaBH_4$ (blue line). (b) XRD pattern of the hydrolysis byproduct of the purified product.

Fig. 3b shows the solid-state ^{11}B MAS NMR spectra of boron compounds produced during ball milling and depending on different milling times. When the milling time changes from 1 to 2 h, the intensity of $[B(OH)_4]^-$ resonance decreases sharply, while the intensity of $[BH_4]^-$ resonance increases, indicating the conversion from $[B(OH)_4]^-$ to $[BH_4]^-$. Due to the self-supplied H from the $[OH]^-$ group in the raw material of $NaB(OH)_4$, and the avoiding of high temperature dehydration in this system, the cost of the regenerated $NaBH_4$ is significantly reduced, which is benefited from the implication of the $Mg_{17}Al_{12}$ alloy. From price calculations of the raw materials, the expected costs of this process is ~20 fold lower than the method using MgH_2 and dehydrated $NaBO_2$ as raw materials (Table S1). Around 25% of raw materials cost drop is also achieved compared with the commercial method.

3.4 Hydrolysis

The generation of hydrogen from produced $NaBH_4$ via hydrolysis was also examined to confirm its property. Here, a low cost and effective non-noble metal catalyst, cobalt chloride $(CoCl_2)^{28}$, was used in the hydrolysis process. According to the hydrogen generation curves in Fig. 4a, the regenerated $NaBH_4$ shows a fast kinetics of hydrogen generation, although with a little lower final hydrogen generation content than the commercial $NaBH_4$ one. Nevertheless, around 2215 mL g^{-1} hydrogen can be generated within 10 min, with a conversion rate of about 86 %. After the hydrolysis, the byproduct was collected and placed in ambiance condition for 48 h before XRD measurement. In the XRD pattern (Fig. 4b), the low intensity diffraction peaks

regeneration process of spent $NaBH_4$. Using the inexpensive $Mg_{17}Al_{12}$ alloy, a H^--anion in the regenerated $NaBH_4$ is directly transferred from the $[OH]^-$ group to H^-. The yield in $NaBH_4$ reaches 72 %, which results from the reducibility Mg and also Al metal. During the reduction process, firstly the $Mg_{17}Al_{12}$ alloy reacts with $NaB(OH)_4$ and generates $NaBH_4$, MgO and Al-metal. Afterwards Al-metal reacts with residual $NaB(OH)_4$ and produces $NaBH_4$ and Al_2O_3. Since both metals of the cheap $Mg_{17}Al_{12}$ alloy can act as a reduction agent the commercial costs of this regeneration method is further reduced by a factor of ~20 compared to regeneration methods using metal hydrides as reducing agent. This indicates a promising commercialization regeneration process and could open a door for broad applications of energy supply from $NaBH_4$.

Acknowledgement

Reference

1. U. Eberle, B. Muller and R. von Helmolt, *Energy Environ Sci.*, 2012, **5**, 8780-8798.

Journal of Materials Chemistry A Accepted Manuscript

2.   S. Guo, J. Sun, Z. Zhang, A. Sheng, M. Gao, Z. Wang, B. Zhao and W. Ding, *J Mater. Chem. A*, 2017, **5**, 15879-15890.

3.   S. Park, J. M. Vohs and R. J. Gorte, *Nature*, 2000, **404**, 265.

4.   D. M. F. Santos and C. A. C. Sequeira, *Renewable and Sustainable Energy Rev*, 2011, **15**, 3980-4001.

5.   G. Rostamikia and M. J. Janik, *Energy Environ. Sci.*, 2010, **3**, 1262-1274.

6.   U. B. Demirci, O. Akdim and P. Miele, *Int. J. Hydrogen Energy*, 2009, **34**, 2638-2645.

7.   I. Merino-Jiménez, C. Ponce de León, A. A. Shah and F. C. Walsh, *J. Power Sources*, 2012, **219**, 339-357.

8.   A. Marchionni, M. Bevilacqua, J. Filippi, M. G. Folliero, M. Innocenti, A. Lavacchi, H. A. Miller, M. V. Pagliaro and F. Vizza, *J. Power Sources*, 2015, **299**, 391-397.

9.   M. A. Budroni, S. Garroni, G. Mulas and M. Rustici, *J. Phys. Chem. C*, 2017, **121**, 4891-4898.

10. L. J. Csetenyi, F. P. Glasser and R. A. Howie, *Acta Crystallographica Section C*, 1993, **49**, 1039-1041.

11. Z. P. Li, B. H. Liu, K. Arai and S. Suda, *J. Alloys Compd.*, 2005, **404-406**, 648-652.

12. A. M. Beaird, P. Li, H. S. Marsh, W. A. Al-Saidi, J. K. Johnson, M. A. Matthews and C. T. Williams, *Ind. Eng. Chem. Res.*, 2011, **50**, 7746-7752.

13. Y. Kojima and T. Haga, *Int. J. Hydrogen Energy*, 2003, **28**, 989-993.

14. C.-L. Hsueh, C.-H. Liu, B.-H. Chen, C.-Y. Chen, Y.-C. Kuo, K.-J. Hwang and J.-R. Ku, *Int. J. Hydrogen Energy*, 2009, **34**, 1717-1725.

15. L. Kong, X. Cui, H. Jin, J. Wu, H. Du and T. Xiong, *Energy Fuels*, 2009, **23**, 5049-5054.

16. Ç. Çakanyıldırım and M. Gürü, *Renew. Energ.*, 2010, **35**, 1895-1899.

17. Z. P. Li, B. H. Liu, J. K. Zhu, N. Morigasaki and S. Suda, *J Alloys Compd.*, 2007, **437**, 311-316.

18. B. Liu, *Int. J. Hydrogen Energy*, 2008, **33**, 1323-1328.

19. B. H. Liu, Z. P. Li and S. Suda, *J. Alloys Compd.*, 2009, **474**, 321-325.

20. B. H. Liu, Z. P. Li and J. K. Zhu, *J Alloys Compd.*, 2009, **476**, L16-L20.

21. D. A. Lyttle, E. H. Jensen and W. A. Struck, *Anal. Chem.*, 1952, **24**, 1843-1844.

22. L. Ouyang, M. Ma, M. Huang, R. Duan, H. Wang, L. Sun and M. Zhu, *Energies*, 2015, **8**, 4237.

23. C. Suryanarayana, *Prog. Mater. Sci.*, 2001, **46**, 1-184.

24. H. Zhong, L. Z. Ouyang, J. S. Ye, J. W. Liu, H. Wang, X. D. Yao and M. Zhu, *Energy Storage Materials*, 2017, **7**, 222-228.

25. W. Chen, L. Z. Ouyang, J. W. Liu, X. D. Yao, H. Wang, Z. W. Liu and M. Zhu, *J. Power Sources*, 2017, **359**, 400-407.

26. H. Zhong, L. Ouyang, J. Liu, C. Peng, X. Zhu, W. Zhu, F. Fang and M. Zhu, *J. Power Sources*, 2018, **390**, 71-77.

27. L. Ouyang, W. Chen, J. Liu, M. Felderhoff, H. Wang and M. Zhu, *Adv. Energy Mater.*, 2017, 1700299-n/a.

28. H.-B. Dai, G.-L. Ma, X.-D. Kang and P. Wang, *Catal. Today*, 2011, **170**, 50-55.